7.
Surface OZONE
(O_3)

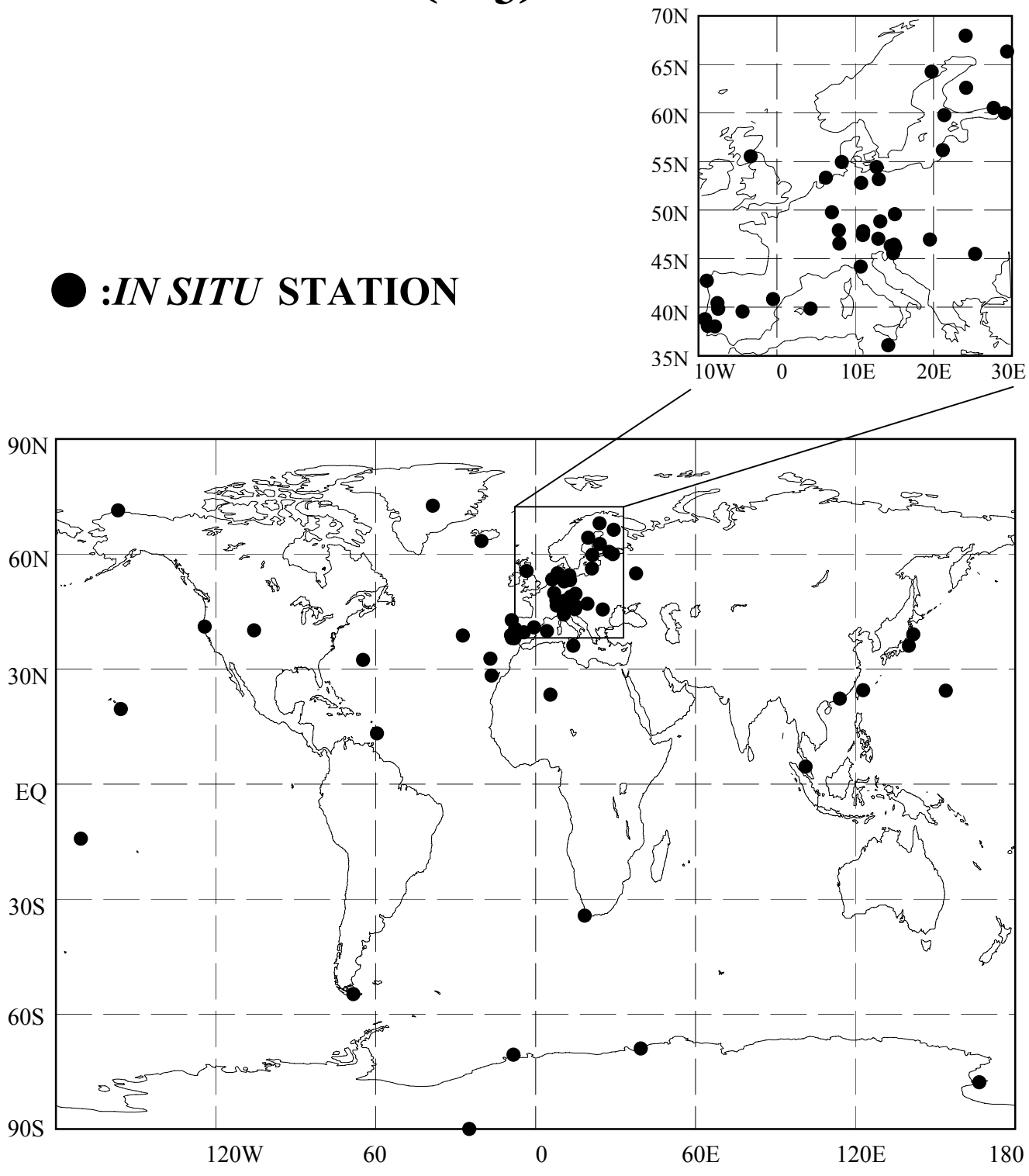

7. Surface Ozone (O_3)

Ozone plays an important role in the atmospheric environment through radiative and chemical processes. Ozone absorbs UV radiation in the stratosphere, and this energy influences the temperature profile and circulation in the stratosphere. Ozone also absorbs IR radiation, and is thus one of the greenhouse gases in the troposphere. However, ozone differs greatly from other greenhouse gases (such as CO_2, CH_4, N_2O and CFCs). Ozone does not have direct natural sources, but rather is produced in the atmosphere, and its concentration ranges from around 10 ppb near the remote Earth's surface to about 10 ppm in the stratosphere. In contrast to ozone, CO_2, CH_4, N_2O and halocarbons (e.g., CFCs) are relatively uniform, hence the term "well-mixed greenhouse gases".

A variation in ozone near the Earth's surface (so-called surface ozone) reflects various reactions involving ozone. Tropospheric ozone is partly transported from the stratosphere; the rest is chemically produced in the troposphere itself, especially near the Earth's surface, where various ozone precursors are emitted. At the same time, ozone is destroyed mainly through chemical reactions with OH radicals and deposition at the Earth's surface.

Ozone is produced in the troposphere through oxidation of precursors, i.e., CO or hydrocarbons in the presence of high concentrations of NO_x. As will be mentioned in following chapters, these substances (so-called "ozone precursors") are anthropogenic. As they are localized and their lifetimes are generally short, the distribution of surface ozone, produced from anthropogenic precursors, is also localized and time-variant.

Surface ozone is estimated to have increased since pre-industrial times (IPCC, 2001).

The World Data Centre for surface ozone was transferred from NILU to JMA in August 2002. Observation stations that submit surface O_3 data to the WDCGG are shown on the map at the beginning of this chapter.

Plate 7.1 shows the time series of monthly mean concentrations of surface O_3 for individual stations, colour-coded to indicate the concentration level. Please note that the data on surface O_3 is reported in two units, namely mixing ratio (ppb) and weight per volume ($\mu g/m^3$) at 25°C. Weights per volume ($\mu g/m^3$) are converted to mixing ratios (ppb) as follows:

X_p [ppb] = ($R * T / M / P_0$) * 10 * X_g [$\mu g/m^3$]

where R is the molar gas constant (8.31451 [J/K/mol]),
T is the absolute temperature reported by an individual station,
M is the molecular weight of O_3 (47.9982), and
P_0 is the standard pressure (1013.25 [hPa]).

The concentration of surface O_3 varies from station to station, many of which are located in Europe. Moreover, the seasonal and interannual variation is relatively large at most stations so that it is difficult to identify a general long-term trend for surface O_3 concentrations.

Figures 7.1 and 7.2 show averaged seasonal cycles from which the long-term trends are subtracted for each 30° latitudinal zone of a single- or multi-peak type. The seasonal cycles for

each site are separable into two types: a single-peak type that has a maximum monthly mean and a multi-peak type that has more than one annual maximum. One single-peak type, the Southern Hemisphere site is not shown in Figure 7.1. The maximum concentration of the single-peak type appears in April in northern high and low latitudes and in May in northern mid-latitudes. The delayed peak in the mid-latitudes may be attributed to the air pollution in Europe given that most mid-latitude stations are located in Europe. Relatively high spring maximum concentrations are observed at Sonnblick, Niwot Ridge, Assekrem, and Mauna Loa, all of which are located at high altitude (higher than 2700 m).

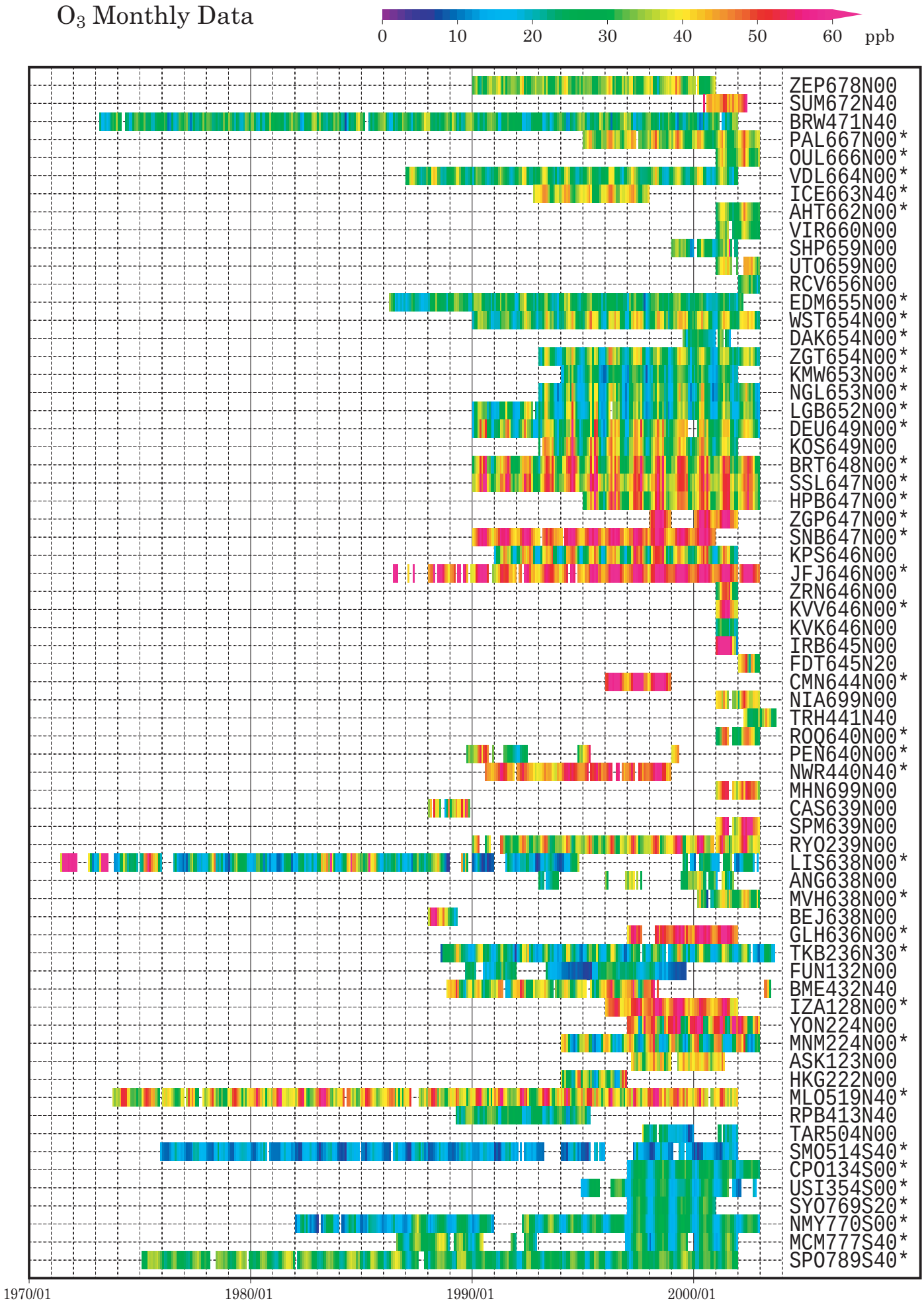

Plate 7.1 Monthly mean concentrations of surface ozone for all stations reported to the WDCGG. The stations are set from north to south. It is shown that an asterisk incidental to station index is one peak type in the analysis shown in Fig 7.1.

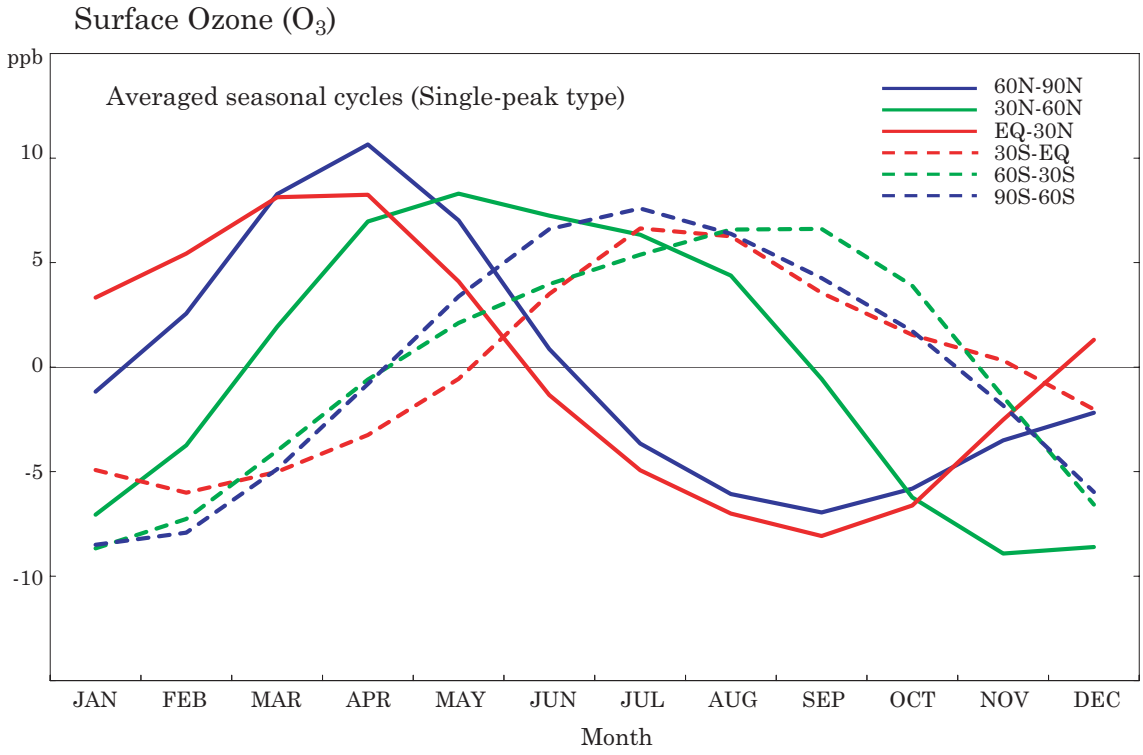

Fig. 7.1 Averaged seasonal cycles of single-peak type for each 30° latitudinal zone from which the long-term trands were subtracted.

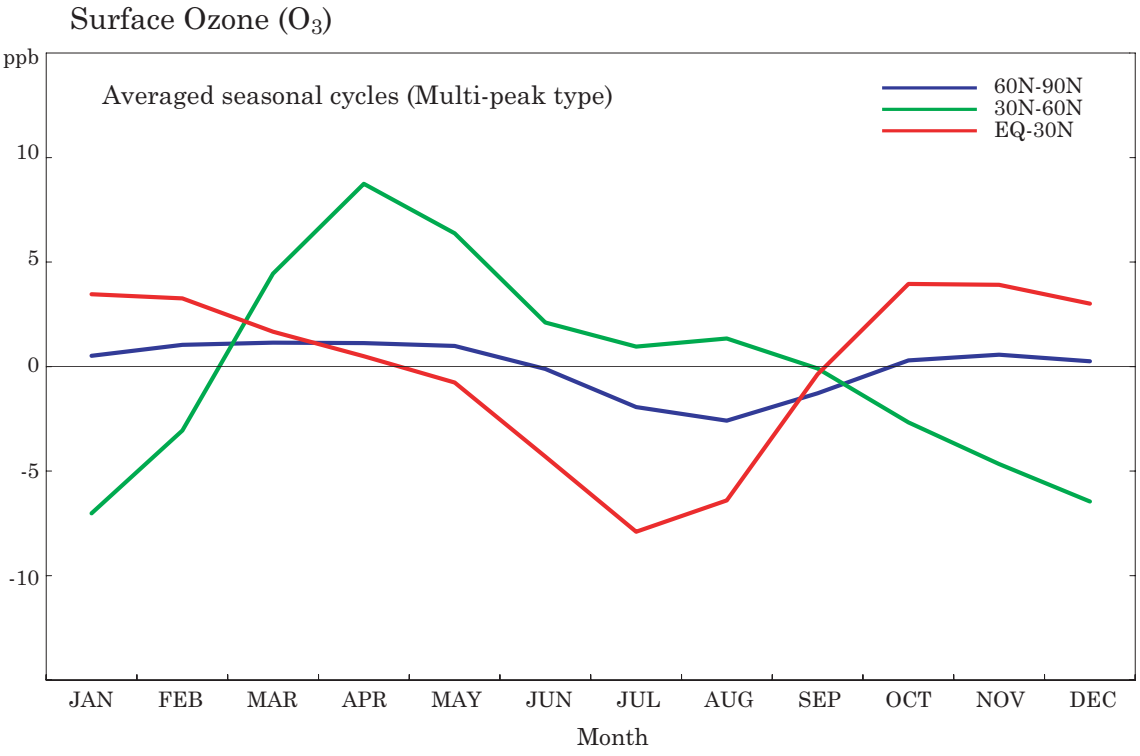

Fig. 7.2 Averaged seasonal cycles of multi-peak type for each 30° latitudinal zone from which the long-term trands were subtracted.